Supplementary Information (SI) for New Journal of Chemistry.
This journal is © The Royal Society of Chemistry and the Centre National de la Recherche Scientifique 2026

Supporting Information

Construction of Mo-doped NiFe-LDH/NiCoP heterostructure electrocatalyst for enhancing urea-assisted overall water splitting performance

Longfei Wang[a], Aize Hao[b,*], Yali Cao[a], Zhenjiang Lu[a], Jindou Hu[a], Jing Xie[a,*], Jiajie Huang[b], Linhui Li[b] and Huiling Ma[b]

[a] State Key Laboratory of Chemistry and Utilization of Carbon Based Energy Resources, College of Chemistry, Xinjiang University, Urumqi 830017, P. R. China

[b] School of Chemical Engineering, Sichuan University of Science and Engineering, Zigong 643000, P. R. China

Corresponding Author

* E-mail: h1061717965@163.com (A. Hao); xiejing@xju.edu.cn (J. Xie).

Experimental Section

S1. Materials and chemicals

All the chemicals were used as received without further purification. $Na_2MoO_4 \cdot 2H_2O$ (A.R., 99.0%)，$Fe(NO_3)_3 \cdot 9H_2O$ (A.R., 99.0%) and $Co(NO_3)_2 \cdot 6H_2O$ (A.R., 99.0%) were supplied by Adamas-beta (Shanghai). $NiCl_2 \cdot 6H_2O$ (A.R., 99.0%) was purchased from Tianjin Fengchuan Chemical Reagent. NH_4F (99.0%)，$CO(NH_2)_2$ (99.0%) was obtained from Aladdin.

S2. Synthesis of NiFe-LDH/NF and Mo-NiFe-LDH/NF

NiFe-LDH/NF: 0.2419 g of $NiCl_2 \cdot 6H_2O$, 0.3636 g of $Fe(NO_3)_3 \cdot 9H_2O$, 0.1111 g of NH_4F and 0.3003 g of urea were added to a mixed solution of 25 mL of deionized water and 5 mL of absolute ethanol. The mixture was magnetically stirred for 1 h to obtain a clear and transparent turquoise solution. The obtained solution and one piece of nickel foam (NF, 2×3 cm^2) were transferred into a 50 mL autoclave, and a hydrothermal reaction was carried out at 120 °C for 8 h. After naturally cooling to room temperature, the NiFe-LDH/NF sample was collected, washed alternately with deionized water and absolute ethanol, and dried in vacuum at 60 °C for 12 h to obtain the NiFe-LDH/NF sample.

Mo-NiFe-LDH/NF: 0.2419 g of $NiCl_2 \cdot 6H_2O$, 0.3636 g of $Fe(NO_3)_3 \cdot 9H_2O$, 0.012 g of $Na_2MoO_4 \cdot 2H_2O$, 0.1111 g of NH_4F and 0.3003 g of urea were added to a mixed solution of 25 mL of deionized water and 5 mL of absolute ethanol. The mixture was magnetically stirred for 1 h to obtain a clear and transparent turquoise solution. The obtained solution and one piece of nickel foam (NF, 2×3 cm^2) were transferred into a 50 mL autoclave, and a hydrothermal reaction was carried out at 120 °C for 8 h. After naturally cooling to room temperature, the Mo-NiFe-LDH/NF sample was collected,

washed alternately with deionized water and absolute ethanol, and dried in vacuum at 60 °C for 12 h to obtain the Mo-NiFe-LDH/NF sample.

S3. Synthesis of NiCoP/NF

First, 0.87 g of $Co(NO_3)_2·6H_2O$ and 0.3 g of urea were completely dissolved in 30 mL of deionized water. Then, the solution was transferred into a 50 mL Teflon autoclave containing a piece of nickel foam (2 cm × 3 cm), where the nickel foam served as the Ni source. Subsequently, the autoclave was sealed and maintained at 120 °C for 6 h. After the autoclave was cooled to room temperature, the precursor was collected, washed several times with water and ethanol, and then dried at 60 °C for 12 h. Finally, it was placed downstream in a high-temperature tube furnace, and 120 mg of NaH_2PO_2 powder was placed at the upstream position. Then, the tube furnace was heated from room temperature to 350 °C at a rate of 3 °C/min in an Ar atmosphere, maintained for 2 h, and then cooled to room temperature to obtain NiCoP/NF.

S4. Synthesis of Mo-NiFe-LDH/NiCoP/NF

The 0.2419 g of $NiCl_2·6H_2O$, 0.3636 g of $Fe(NO_3)_3·9H_2O$, 0.012 g of $Na_2MoO_4·2H_2O$, 0.1111 g of NH_4F and 0.3003 g of urea were added to a mixed solution of 25 mL of deionized water and 5 mL of absolute ethanol. The mixture was magnetically stirred for 1 h to obtain a clear and transparent turquoise solution. The obtained solution and one piece of above NiCoP/NF (2×3 cm^2) were transferred into 50 mL reaction kettle. A hydrothermal reaction was carried out at 120 °C for 8 h. After naturally cooling to room temperature, the Mo-NiFe-LDH/NiCoP/NF sample was collected, washed alternately with deionized water and absolute ethanol, and dried in vacuum at 60 °C for 12 h to obtain the Mo-NiFe-LDH/NiCoP/NF sample.

S5. Synthesis of Pt-C/NF and RuO_2/NF

Briefly, 2.5 mg of Pt-C, add 490 μL of dispersion (anhydrous ethanol: deionized water = 1:1), 10 μL of Nafion, sonicated for 1 h to obtain a uniformly dispersed ink. Taking 20 μL of ink, uniformly dropped onto NF, and dried at room temperature to obtain Pt-C/NF. The preparation of RuO_2/NF was carried out uniformly as shown above except that Pt-C was replaced by RuO_2, and the loading of RuO_2/NF and Pt-C/NF was 0.1 mg cm^{-2}.

S6. Electrochemical performances measurements

All electrochemical tests were conducted by using CHI 760E electrochemical work station at room temperature. The Hg/HgO served as the reference electrode, a Pt sheet functioned as the counter electrode, and the catalysts themselves were employed as the working electrode. Hydrogen evolution reaction (HER), oxygen evolution reaction (OER) and overall water splitting tests occurred in 1 M KOH solution. Urea oxidation reaction (UOR) and urea-assisted water splitting tests were carried out in a mixed solution of 1 M KOH and 0.5 M urea. The all potentials of tests which were corrected to the reversible hydrogen electrode (RHE) by using the following equation: $E\ (RHE) = E\ (Hg/HgO) + 0.098 + 0.0591*pH$. Stability tests were obtained by performing 3000 CV cycles and by the constant current method. Linear sweep voltammetry polarization curves and Tafel slopes were obtained at a scan rate of 5 mV s^{-1}. All polarization curves were performed IR compensation with 90 % unless noted otherwise.

The electrochemical surface area (ECSA) of the catalyst was evaluated by electrical double–layer capacitance (C_{dl}):

$$ECSA = C_{dl}/C_s\ cm^2. \quad (1)$$

C_{dl} values were computed by cyclic voltammetry (CV) scanning between non–Faraday regions at scan rates from $20\ mV\ s^{-1}$ to $100\ mV\ s^{-1}$. Electrochemical impedance spectroscopy (EIS) was collected at an amplitude of 5 mV as well as frequency range of 10^5 to $0.01\ Hz$. In situ EIS test voltage range of -0.02 to $-0.34\ V\ (vs.\ RHE)$.

To calculate the turnover frequency (TOF), CV measurements was conducted in 1

M PBS (pH = 7) in the potential range of *-0.2 ~ 0.6 V* (vs. RHE) at a scan rate of 50 mV s^{-1}. Here, assuming that almost all surface-active sites are accessible to the electrolyte, it is possible to evaluate TOF values in HER, OER and UOR by the following equation:

$$TOF = I/2nF \ (HER) \quad (2)$$

$$TOF = I/4nF \ (OER) \quad (3)$$

$$TOF = I/6nF \ (UOR) \quad (4)$$

Here, I was the current (A) during the LSV measurement at a selected overpotential (0.2 V vs. RHE) in HER, F is the faraday constant (96485 C/mol), and n is the number of moles of the active sites. In this $2e^-$ HER, $4e^-$ OER, and $6e^-$ UOR, n can be calculated by the following equation:

$$n=Q/2F \quad (5)$$

Here, F and Q correspond to the Faraday constant (96485 C/mol) and the whole charge of CV curve (C), respectively.

Figures

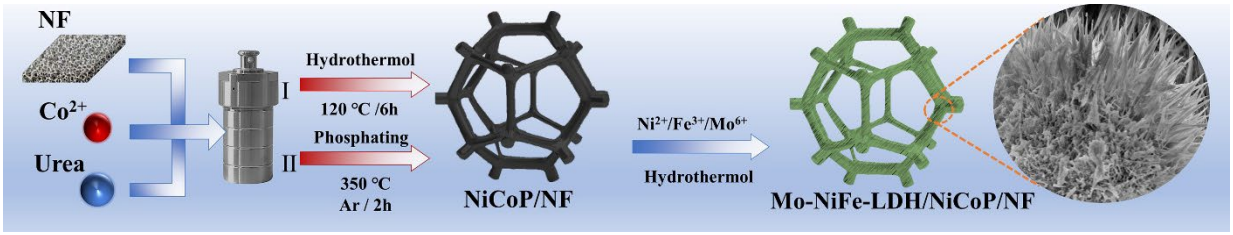

Fig. S1 Schematic illustration of synthetic procedures of Mo-NiFe-LDH/NiCoP/NF electrocatalyst.

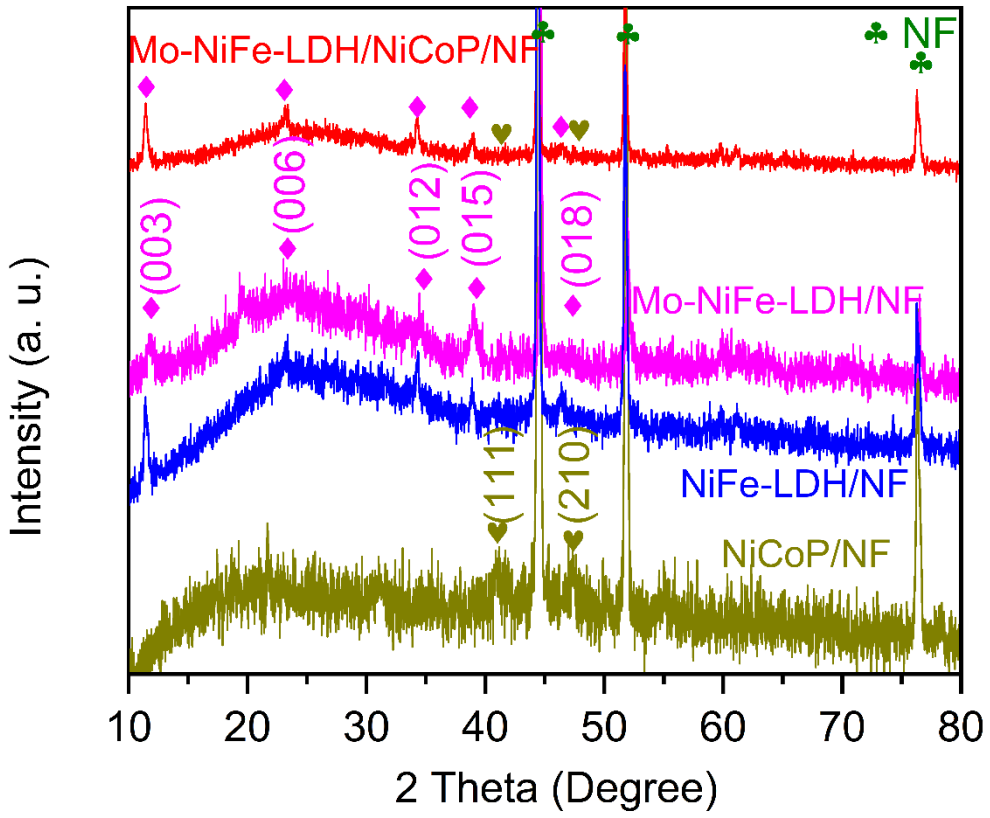

Fig. S2 XRD patterns of NiCoP/NF, NiFe-LDH/NF and Mo-NiFe-LDH/NF and Mo-NiFe-LDH/NiCoP/NF.

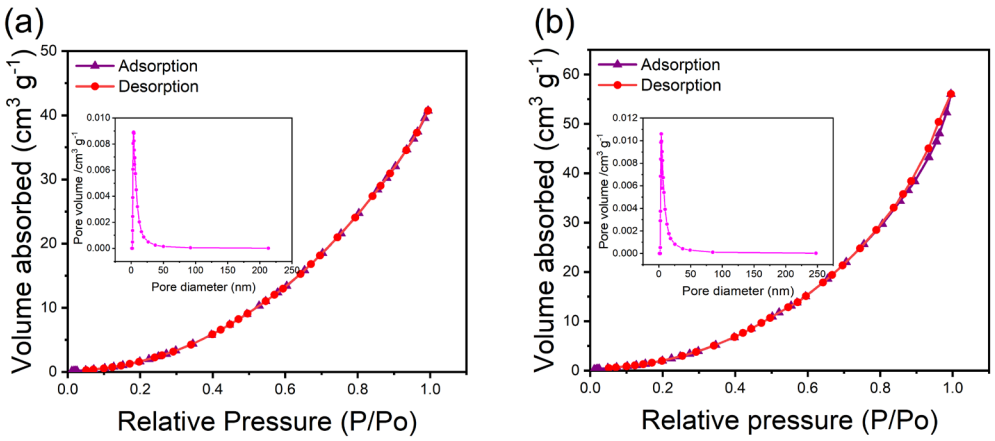

Fig. S3 Nitrogen adsorption−desorption isotherms and pore-size distributions of (a) NiCoP/NF and (b) Mo-NiFe-LDH/NiCoP/NF.

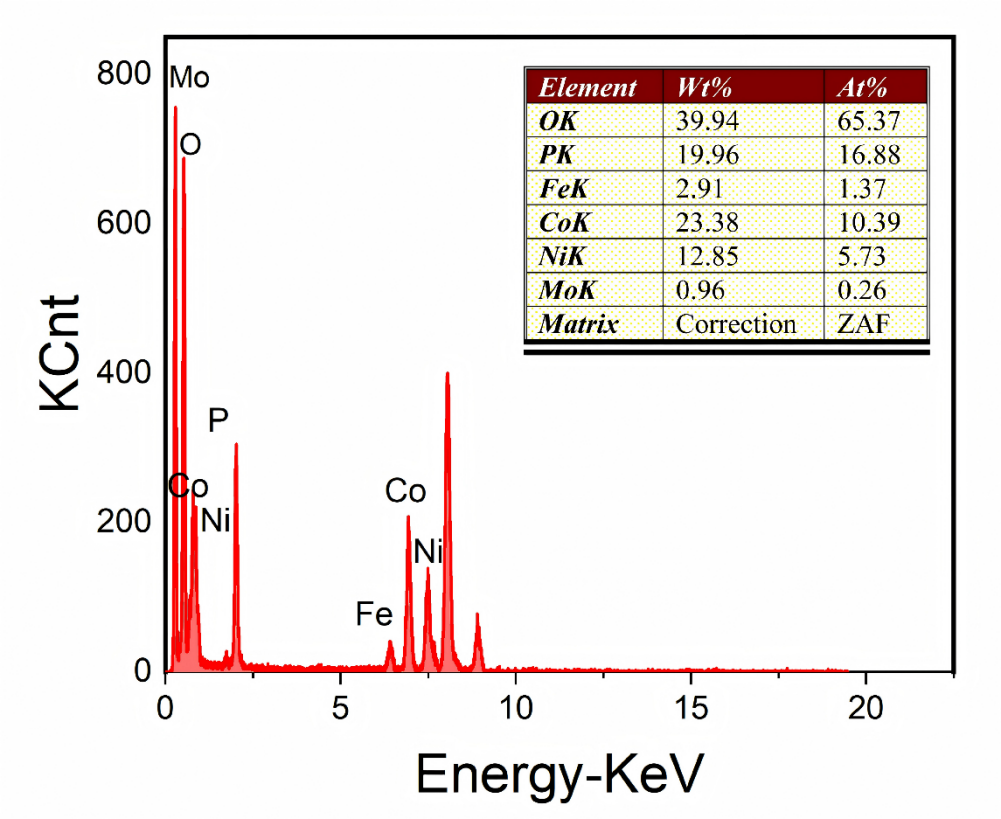

Fig. S4 EDS image of Mo-NiFe-LDH/NiCoP/NF.

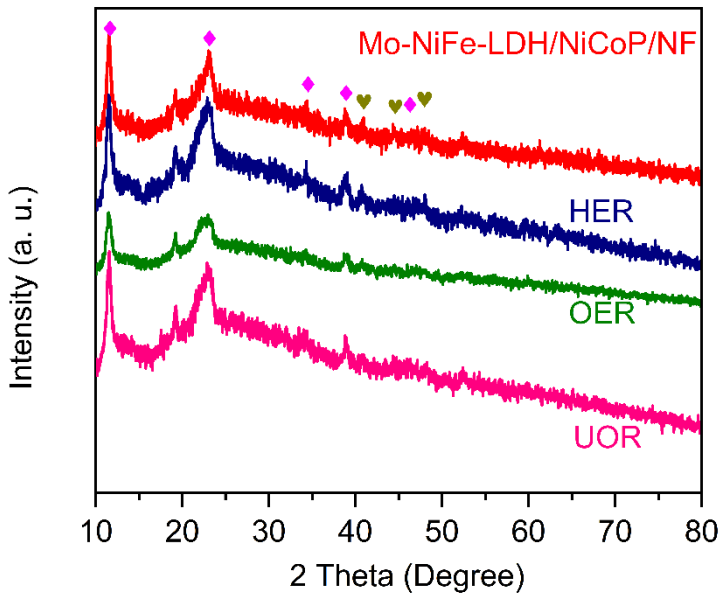

Fig. S5 XRD images of Mo-NiFe-LDH/NiCoP/NF after HER, OER and UOR stability test.

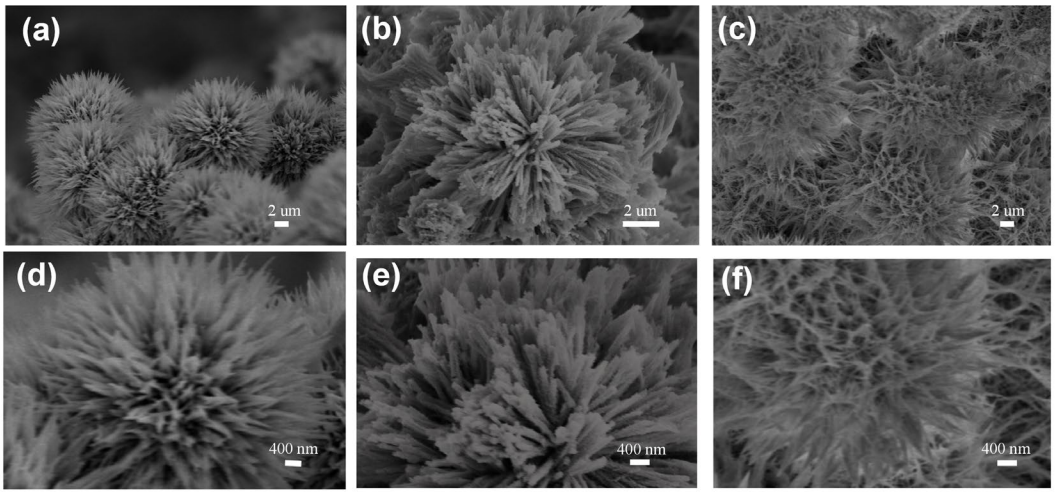

Fig. S6 SEM images of Mo-NiFe-LDH/NiCoP/NF after (a, d) HER, (b, e) OER and (c, f) UOR stability test.

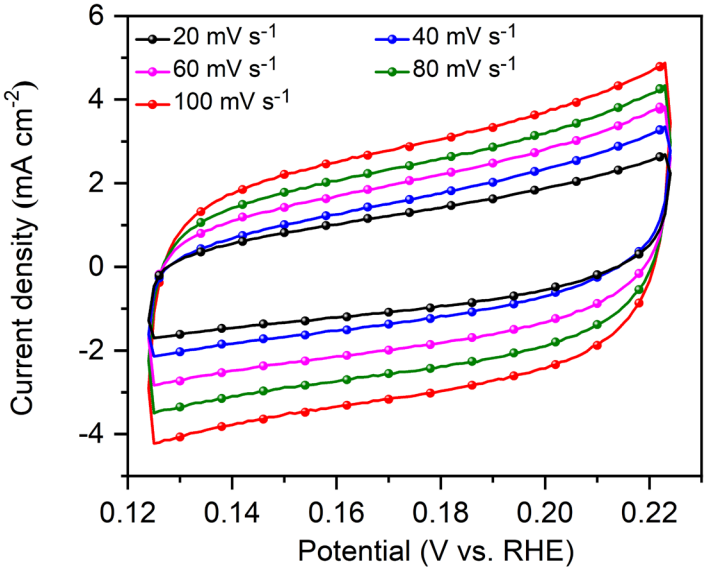

Fig. S7 HER cyclic voltammograms of NiFe-LDH/NF at different scan rates of 20, 40, 60, 80 and 100 mV s^{-1}.

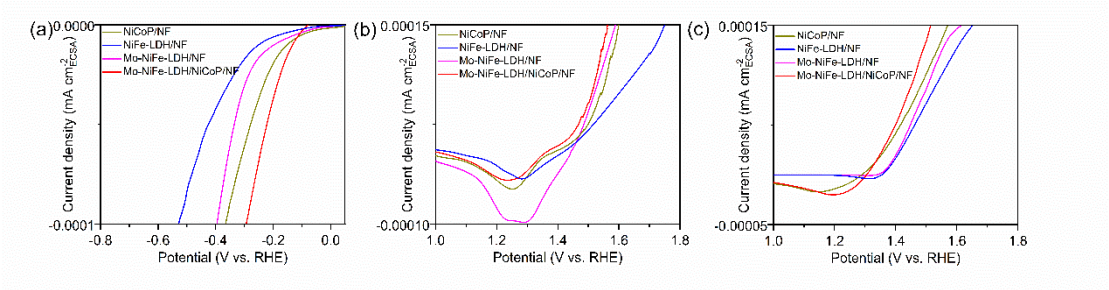

Fig. S8 ECSA normalized LSV curves for Mo-NiFe-LDH/NiCoP/NF, NiCoP/NF, NiFe-LDH/NF and Mo-NiFe-LDH/NF in (a) HER, (b) OER and (c) UOR.

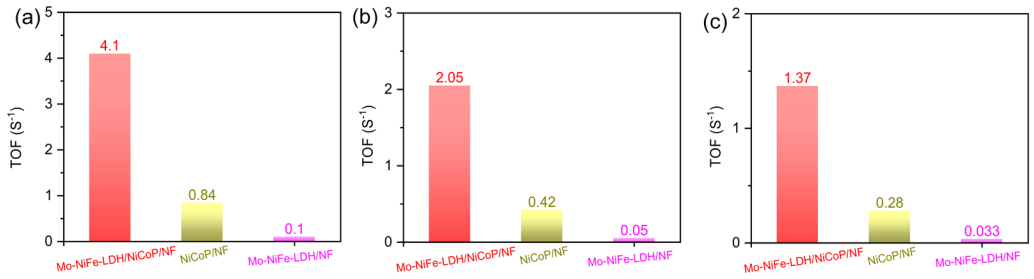

Fig. S9 TOF histogram at 200 mV of Mo-NiFe-LDH/NiCoP/NF, NiCoP/NF and Mo-NiFe-LDH/NF in (a) HER, (b) OER and (c) UOR.

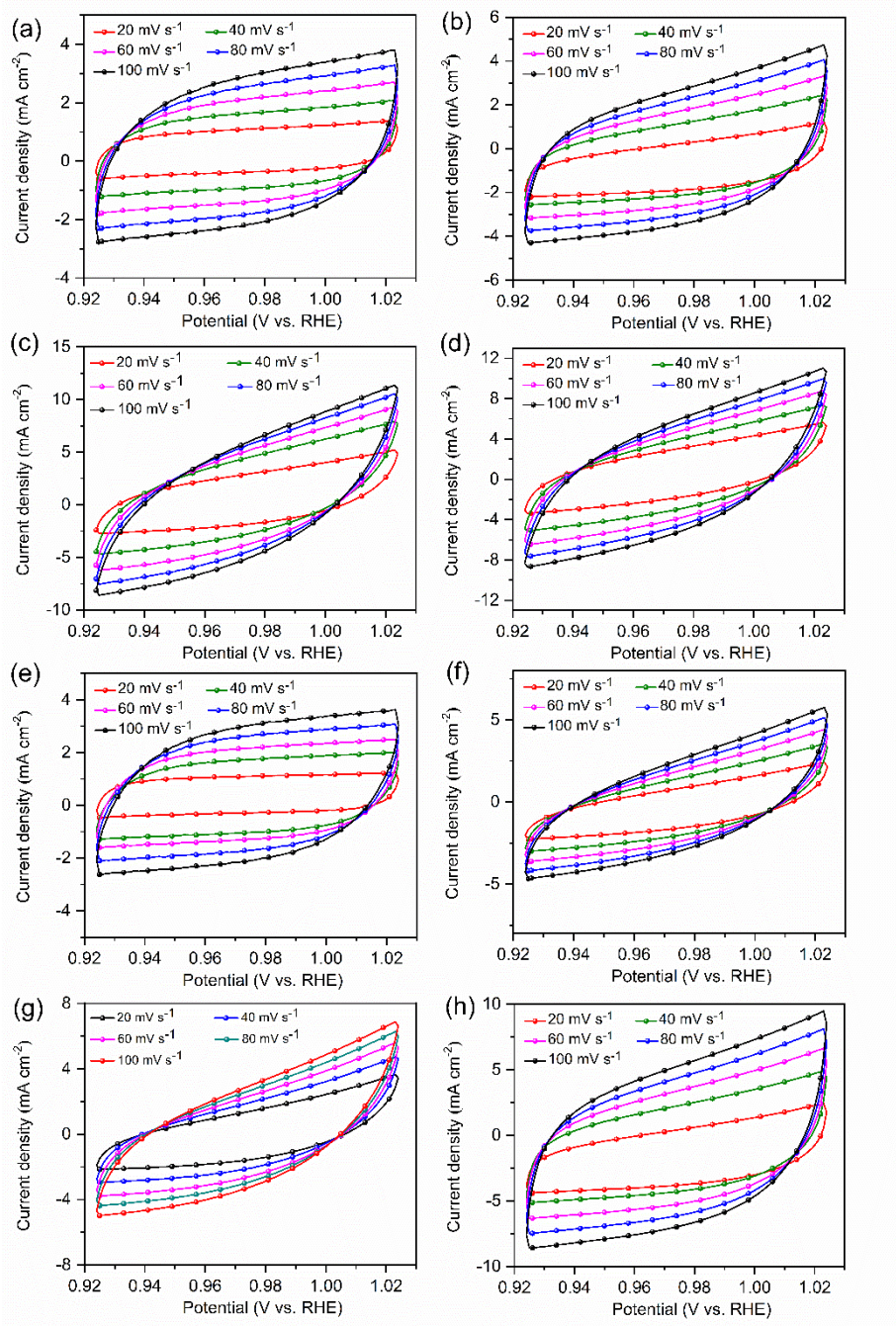

Fig. S10 OER cyclic voltammograms (CV) for (a) NiFe-LDH/NF (b) Mo-NiFe-LDH/NF, (c) NiCoP/NF and (d) Mo-NiFe-LDH/NiCoP/NF at different scan rate with 20, 40, 60, 80 and 100 mV s^{-1}. UOR cyclic voltammograms (CV) for (e) NiFe-LDH/NF (f) Mo-NiFe-LDH/NF, (g) NiCoP/NF and (h) Mo-NiFe-LDH/NiCoP/NF at different scan rate with 20, 40, 60, 80 and 100 mV s^{-1}.

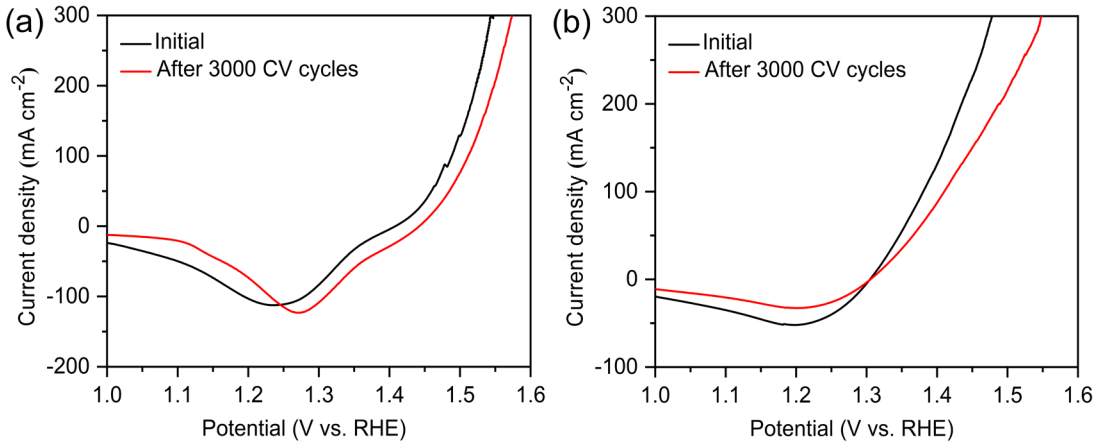

Fig. S11 (a-b) Polarization curves of Mo-NiFe-LDH/NiCoP/NF at initial and after 3000 CV scans for OER and UOR, respectively.

Fig. S12 Optical photographs of H_2 and O_2 collected by drainage method.

Table S1. Comparison of the HER electrocatalytic performance of Mo-NiFe-LDH/NiCoP/NF catalysts with recently reported electrocatalysts in 1 M KOH.

Catalysts	Current Density (j mA cm^{-2})	Overpotential at Corresponding j (mV)	Reference
Ni_2P-CoP	10	102	[1]
$Ni_{1.85}Fe_{0.15}P$/NF	10	106	[2]
s−CoP/Co_3O_4	10	116	[3]
CoP/Ti−2.0	10	116	[4]
CoP@MoS_2	10	119	[5]
$CoMoO_4$−CoP/NC	10	122	[6]
CoP@Ni/Fe−P/CC	10	125	[7]
$NiCo_2S_4$/Ni_3S_2/NF	10	127	[8]
C-(Fe-Ni)P@PC /(Ni-Co)P@CC	10	142	[9]
$FeCoP_2$@NPPC	10	150	[10]
NiFeP@C	10	160	[11]
$NiCo_2N$/NF	10	180	[12]
NiFeP@N-CS	10	186	[13]
$NiCo_2S_4$ NW/NF	10	210	[14]
Ni_2P-FeP	10	250	[15]
Mo-NiFe-LDH/NiCoP/NF	10	104	This work

Table S2. Comparison of the OER electrocatalytic performance of Mo-NiFe-LDH/NiCoP/NF catalysts with the recently reported electrocatalysts in 1 M KOH.

Catalysts	Current Density (j mA cm^{-2})	Overpotential at Corresponding j (mV)	Reference
P-NiFeW	10	188	[16]
NiFeCe-LDH/NF	10	232	[17]
NiCo/Fe_3O_4/MOF-74	10	238	[18]
NiFe-20-H/NF	10	241	[19]
H-CMS_x@NiFe LDH/NF	10	253	[20]
Ni_2P-$NiFe_2O_4$/CP	10	255	[21]
$NiCo(OH)_2$/NiS_2 CHCs	10	258	[22]
NiCo@CuO	10	262	[23]
NiCoP/FeNiCoP	10	266	[24]
N-Ni_2Co_3-P	10	290	[25]
NiFe-LDH/PSS/CP	10	282	[26]
$NiWO_4$@$NiSe_2$/NF	10	258	[27]
$Co(OH)_2$/Fe_7Se_8	10	278	[28]
Co-P/Fe_3O_4	20	343	[29]
MoS_2-NiS_2/NGF	10	370	[30]
Mo-NiFe-LDH/NiCoP/NF	10	194	This work

Table S3. Comparison of the overall water splitting performance of Mo-NiFe-LDH/NiCoP/NF with recently reported electrocatalysts in 1 M KOH.

Catalysts	Current Density ($mA\ cm^{-2}$)	Applied voltage (V)	Reference
Fe-CoP/$Ni(OH)_2$	10	1.52	[31]
O-CoP	10	1.54	[32]
CoP/NF	10	1.54	[33]
Ru@FeCoP	50	1.54	[34]
Ru-NCO	10	1.55	[35]
CoMo@CN	10	1.74	[36]
CoP/ NCNHP	10	1.64	[37]
Co/β-Mo_2C@NCNTs	10	1.64	[38]
FeCoP	10	1.68	[39]
CoP@FeCoP/NC YSMPs	10	1.68	[40]
FeOOH/Ni_3S_2-II	10	1.60	[41]
NiFe-LDH/Cu_3P	10	1.75	[42]
NiFe-Se/C	10	1.68	[43]
Ni–Fe–P/Co–P/NF	10	1.61	[44]
$CoCO_3$@NiFe LDH	10	1.78	[45]
NiFe LDH@CoP/NiP_3	10	1.64	[46]
CoP/rGO-400	10	1.70	[47]
Mo-NiFe-LDH/NiCoP/NF	10	1.53	This work

Table S4. Comparison of the urea−assisted overall water splitting performance of Mo-NiFe-LDH/NiCoP/NF catalysts with recently reported electrocatalysts in 1 M KOH + 0.5 M urea electrolytes.

Catalysts	Current Density ($mA\ cm^{-2}$)	Applied voltage (V)	Reference
Rh_{SA}−S−Co_3O_4	10	1.33	[48]
CoFeCr LDH/NF	10	1.33	[49]
CoSeP/CoP	10	1.36	[50]
O-NiMoP/NF	10	1.36	[51]
NF/NiMoO-Ar	10	1.38	[52]
Ni_3S_2−Ni_3P/NF	10	1.43	[53]
FeOOH@Co_3O_4	10	1.43	[54]
CoNiFeS−OH	10	1.46	[55]
NiFeCoSx@ $FeNi_3$	10	1.54	[56]
Ni@NCNT-4	10	1.56	[57]
Ni_2P	10	1.38	[58]
S-MnO_2	10	1.33	[59]
Graphene-$Ni(OH)_2$	10	1.52	[60]
Ni-Mo-O	10	1.35	[61]
MnO_2/$MnCo_2O_4$/ Ni	10	1.33	[62]
Mo-NiFe-LDH/NiCoP/NF	10	1.34	This work

References

[1] Y. Lu, Y. Deng, S. Lu, Y. Liu, J. Lang, X. Cao and H. Gu, *Nanoscale*, 2019, **11**, 21259-21265.

[2] P. Wang, Z. Pu, Y. Li, L. Wu, Z. Tu, M. Jiang, Z. Kou, I.S. Amiinu and S. Mu, *ACS Appl. Mater. Interfaces*, 2017, **9**, 26001-26007.

[3] X. Li, Y. Liu, Q. Sun, W.-H. Huang, Z. Wang, C.-C. Chueh, C.-L. Chen and Z. Zhu, *Nanoscale*, 2021, **13**, 20281-20288.

[4] Y. Yan, Y. Chen, M. Shao, X. Chen, Z. Yang, J. Wang, H. Chen, L. Ni, G. Diao and M. Chen, *ACS Sustain. Chem. Eng.*, 2023, **11**, 2499-2510.

[5] T. Xia, L. Zhou, S. Gu, H. Gao, X. Ren, S. Li, R. Wang and H. Guo, *Mater. Des*., 2021, **211**, 110165.

[6] J. Luo, Y. Zhou, X. Wang, Y. Gu, W. Liu, S. Wang and J. Zhang, *J. Colloid. Interface Sci*., 2023, **648**, 90-101.

[7] L. Yu, P. Wu, T. Tian, X. He, M. Fan and L. Cui, *Dalton Trans.*, 2023, **52**, 11941-11948.

[8] X. Y. Zhao, H. Liu, Y. Rao, X.X. Li, J. L. Wang, G. S. Xia and M.B. Wu, *ACS Sustain. Chem. Eng*., 2019, **7**, 2610-2618.

[9] C.-N. Lv, L. Zhang, X.-H. Huang, Y.-X. Zhu, X. Zhang, J.-S. Hu and S.-Y. Lu, *Nano Energy*, 2019, **65**, 103995.

[10] Y.-N. Wang, Z.-J. Yang, D.-H. Yang, L. Zhao, X.-R. Shi, G. Yang and B.-H. Han, *ACS Appl. Mater. Interfaces*, 2021, **13**, 8832-8843.

[11] X. Yu, J. Zhao and M. Johnsson, *Adv. Funct. Mater*., 2021, **31**, 2101578.

[12] Y. Wang, B. Zhang, W. Pan, H. Ma and J. Zhang, *ChemSusChem*, 2017, **10**, 4170-4177.

[13] J. Hei, G. Xu, B. Wei, L. Zhang, H. Ding and D. Liu, *Appl. Surf. Sci.*, 2021, **549**,

149297.

[14] A. Sivanantham, P. Ganesan and S. Shanmugam, *Adv. Funct. Mater.*, 2016, **26** 4661-4672.

[15] H. Wang, X. Wang, B. Zheng, D. Yang, W. Zhang and Y. Chen, *Electrochim. Acta*, 2019, **318**, 449-459.

[16] H. Zhang, L. Li, K. Li, C. Yue, L. Dang and G. Liu, *J. Alloys Compd*., 2025, **1049**, 185348.

[17] Y. Liao, R. He, W. Pan, Y. Li, Y. Wang, J. Li and Y. Li, *Chem. Eng. J*., 2023, **464**, 142669.

[18] X. Wang, H. Xiao, A. Li, Z. Li, S. Liu, Q. Zhang, Y. Gong, L. Zheng, Y. Zhu, C. Chen, D. Wang, Q. Peng, L. Gu, X. Han, J. Li and D. Li, J. Am. *Chem. Soc*., 2018, **140**, 15336-15341.

[19] S. Wang, H. Wang, S. Chen, K. K. K. Cheung, H. F. Wong, C. W. Leung and J. A. Zapien, *Int. J. Hydrogen Energy*, 2023, **48**, 17045-17054.

[20] Y. J. Lee and S.-K. Park, *Rare Met.*, 2024, **43**, 522-532.

[21] Y. Li, Z. Zhang, Z. Zhang, J. He, M. Xie, C. Li, H. Lu, Z. Shi and S. Feng, *Appl. Catal., B*, 2023, **339**, 123141.

[22] J. Wang, A. Yang, J. Li, K. Su, Y. Tang and X. Qiu, *Appl. Catal., B*, 2022, **300**, 120727.

[23] B. Chen, Z. Zhang, S. Kim, M. Baek, D. Kim and K. Yong, *Appl. Catal., B*, 2019, **259**, 118017

[24] P. Gao, C. Yue, J. Zhang, J. Bao, H. Wang, Q. Chen, Y. Jiang, S. Huang, Z. Hu and J. Zhang, *J. Colloid Interface Sci*., 2024, **666**, 403-415.

[25] X. Lin, L. Chen, X. Zhong, A. BaQais, W. Dang, M. A. Amin, H. Huang, H. Li, G. Liang and G. Liu, Adv. *Compos. Hybrid Mater*., 2023, **6**, 79.

[26] C.-P. Wang, H. Sun, G. Bian, J.-X. Wang, X. Pang, G. Wang, J. Zhu and X.-H. Bu, *Nano Res*., 2024, **17**, 1114-1122.

[27] J. Li, X. Du and X. Zhang, *J. Alloys Compd*., 2023, **951**, 169941.

[28] C. Gong, L. Zhao, D. Li, X. He, H. Chen, X. Du, D. Wang, W. Fang, X. Zeng and W. Li, *Chem. Eng. J.*, 2023, **466**, 143124.

[29] J. Liu, G. Chen, J. Xiao and Y. Zhang, *Int. J. Hydrogen Energy*, 2024, **62**, 803-811.

[30] P. Kuang, M. He, H. Zou, J. Yu and K. Fan, *Appl. Catal., B*, 2019, **254**, 15-25.

[31] Y. Xu, S. Yin, C. Li, K. Deng, H. Xue, X. Li, H. Wang and L. Wang, *J. Mater. Chem. A*, 2018, **6**, 1376-1381.

[32] R. Dong, A. Zhu, P. Tan, Y. Liu, M. Jiang, L. Yang, J. Xie and J. Pan, *J. Colloid Interface Sci*., 2022, **622**, 239-249.

[33] J. Liu, Y. Gao, X. Tang, K. Zhan, B. Zhao, B. Y. Xia and Y. Yan, *J. Mater. Chem. A*, 2020, **8**, 19254-19261.

[34] Y. Wang, Y. Du, Z. Fu, J. Ren, Y. Fu and L. Wang, *J. Mater. Chem. A*, 2022, **10**, 16071-16079.

[35] J. Zhang, J. Lian, Q. Jiang and G. Wang, *Chem. Eng. J*., 2022, **439**, 135634.

[36] J. Jiang, Q. Liu, C. Zeng and L. Ai, *J. Mater. Chem. A*, 2017, **5**, 16929-16935.

[37] Y. Pan, K. Sun, S. Liu, X. Cao, K. Wu, W.-C. Cheong, Z. Chen, Y. Wang, Y. Li and Y. Liu, *J. Am. Chem. Soc.*, 2018, **140**, 2610-2618.

[38] T. Ouyang, Y. Ye, C. Wu, K. Xiao and Z. Liu, *Angew. Chem., Int. Ed*., 2019, **58**, 4923.

[39] K. Sun, K. Wang, T. Yu, X. Liu, G. Wang, L. Jiang, Y. Bu and G. Xie, *Int. J. Hydrogen Energy*, 2019, **44**, 1328-1335.

[40] J. Shi, F. Qiu, W. Yuan, M. Guo and Z.-H. Lu, *Chem. Eng. J.*, 2021, **403**, 126312.

[41] Q. Guo, X. Liu, C. Ke, W. Xiao and X. Yang, *New J. Chem.* , 2023, **47**, 21732-21742.

[42] H. Wang, T. Zhou, P. Li, Z. Cao, W. Xi, Y. Zhao and Y. Ding, *ACS Sustainable Chem. Eng.*, 2018, **6**, 380-388.

[43] B. Xu, H. Yang, L. Yuan, Y. Sun, Z. Chen and C. Li, *J. Power Sources*, 2017, **366**, 193-199.

[44] H. Wang, W. Li, J. Wu, D. Wang, D. Hou, M. Sheng and R. Guo, *Energy & Fuels*, 2023, **37**, 19103-19112.

[45] R. Que, S. Liu, P. He, Y. Yang and Y. Pan, *Mater. Lett*., 2020, **277**, 128285.

[46] C. Song, Y. Liu, Y. Wang, S. Tang, W. Li, Q. Li, J. Zeng, L. Chen, H. Peng and Y. Lei, *Sci. China Mater.*, 2021, **64**, 1662-1670.

[47] L. Jiao, Y.-X. Zhou and H.-L. Jiang, *Chem. Sci.*, 2016, **7**, 1690-1695.

[48] A. Kumar, X. Liu, J. Lee, B. Debnath, A.R. Jadhav, X. Shao, V.Q. Bui, Y. Hwang, Y. Liu, M.G. Kim and H. Lee, *Energy Environ. Sci*., 2021, **14**, 6494–6505.

[49] Z. Wang, W. Liu, Y. Hu, M. Guan, L. Xu, H. Li, J. Bao and H. Li, *Applied Catalysis B: Environmental*., 2020, **272**, 118959.

[50] B. Lu, C. Lv, Y. Xie, L. Gao, J. Yan, K. Zhu, G. Wang, D. Cao and K. Ye, *Small*, 2023, **19**, 2302923.

[51] H. Jiang, M. Sun, S. Wu, B. Huang, C.S. Lee and W. Zhang, *Adv. Funct. Mater.*, 2021, **31**, 2104951.

[52] Z.-Y. Yu, C.-C. Lang, M.-R. Gao, Y. Chen, Q.-Q. Fu, Y. Duan and S.-H. Yu, *Energy Environ. Sci.*, 2018, **11**, 1890-1897.

[53] J. Liu, Y. Wang, Y. Liao, C. Wu, Y. Yan, H. Xie and Y. Chen, *ACS Applied Materials & Interfaces*., 2021, **13**, 26948-26959.

[54] Q. Zhang, M. Sun, M. Yao, J. Zhu, S. Yang, L. Chen, B. Sun, J. Zhang, W. Hu and

P. Zhao, *J. Colloid. Interface Sci*., 2022, **623**, 617–626.

[55] C. Fang, D. Zhang, X. Wang and R. Li, *Inorg. Chem. Front*., 2022, **9**, 3643–3653.

[56] J. Shen, Q. Li, W. Zhang, Z. Cai, L. Cui, X. Liu and J. Liu, *J. Mater. Chem. A*, 2022, **10**, 5442-5451.

[57] Q. Zhang, F.M. Kazim, S. Ma, K. Qu, M. Li, Y. Wang, H. Hu, W. Cai and Z. Yang, *Appl. Catal., B*, 2021, **280**, 119436.

[58] D. Liu, T. Liu, L. Zhang, F. Qu, G. Du, A. M. Asiri and X. Sun, *J. Mater. Chem. A*, 2017, **5**, 3208-3213.

[59] S. Chen, J. Duan, A. Vasileff and S. Z. Qiao, *Angew. Chem. Int. Ed*., 2016, **55**, 3804-3808.

[60] D. Wang, W. Yan, S. H. Vijapur and G. G. Botte, *Electrochimica Acta*, 2013, **89**, 732-736.

[61] Z.-Y. Yu, C.-C. Lang, M.-R. Gao, Y. Chen, Q.-Q. Fu, Y. Duan and S.-H. Yu, *Energy Environ. Sci*., 2018, **11**, 1890-1897.

[62] C. Xiao, S. Li, X. Zhang and D. R. MacFarlane, *J. Mater. Chem. A*, 2017, **5**, 7825-7832.